Int J Fract (2022) 234:263–272
https://doi.org/10.1007/s10704-021-00589-w

ORIGINAL PAPER

Effect of environmental media on the fatigue property of Chinese A508-3 steel of AP1000

Guangsheng Ning · Weihua Zhong · Jianghua Li · Tao Cong · Jingyu Sun · Hui Wang · Guian Qian · Filippo Berto

Received: 5 May 2021 / Accepted: 27 August 2021 / Published online: 16 September 2021

Abstract The fatigue tests of Chinese RPV steel (A508-3) were carried out under the simulated primary coolant environment of AP1000 which is a kind of 3rd generation nuclear power plant. The effects of temperature, strain rate and dissolved oxygen (DO) on fatigue life were analyzed. During the fatigue test, the material exhibited a cyclic hardening followed by cyclic softening behavior, with no obvious cyclic stability region. In logarithmic coordinates, the S–N curve showed a bilinear relationship. As the strain amplitude increased from 0.2 to 0.6%, the fatigue life approximately decreased from 10^5 to 3×10^2. The environmental correction factor (Fen), which is defined as the ratio of life in air at room temperature to that in the primary coolant environment, decreases as the temperature decreases from 321 to 150 °C. The Fen also decreases as the DO decreases from 0.6 to 0.03 ppm while it increases as the strain rate decreases from 1 to 0.0004%/s. Compared with the NUREG6909 model, the presented model is more applicable for fatigue life prediction of Chinese A508-3 steel.

Keywords Reactor pressure vessel steel · Primary coolant environment · Low cycle fatigue · Corrosion fatigue · Environmental fatigue correction factor

G. Ning · W. Zhong (✉) · H. Wang
China Institute of Atomic Energy, Beijing 102413, China
e-mail: zhongwh@ciae.ac.cn

J. Li · J. Sun (✉) · G. Qian
State Key Laboratory of Nonlinear Mechanics (LNM), Institute of Mechanics, Chinese Academy of Sciences, Beijing 100190, China
e-mail: sunjingyu@imech.ac.cn

T. Cong
Metals & Chemistry Research Institute, China Academy of Railway Sciences Corporation Limited, Beijing 100081, China

F. Berto
Department of Mechanical and Industrial Engineering, Norwegian University of Science and Technology (NTNU), Richard Birkelands vei 2b, 7491 Trondheim, Norway

1 Introduction

The reactor pressure vessel (RPV) is the irreplaceable key component of nuclear power plants (NPPs), which must meet the requirements for Class 1 components according to the ASME standards (Yang 2000; NRC 2007). The ASME Class 1 requirements contain provisions, including fatigue design curves, for determining a component's suitability for cyclic service (S.I. 1992). The fatigue design curve is based on strain-controlled tests performed on small polished specimens at room temperature in air environment. Thus, the curve does not address the impact of the aggressive operation environment (NRC 2007), which

comprises high temperature, high pressure, water coolant, etc. In order to determine the acceptable fatigue life of RPV with consideration of those aggressive operation environments, many countries have carried out fatigue tests of RPV material in simulated primary coolant environments with different parameters (JNES-SS-1005 2011; Chopra and Stevens 2018). Some environmental factors, such as temperature (Byung Ho Lee 1995), strain rate (Higuchi et al. 1298) and dissolved oxygen (DO) (Chopra and Stevens 2018), were considered to be the key affection factor that may cause reduction effects of fatigue life. The reduction effects mechanism in simulated primary coolant environment could be due to the synergistic effect of environmentally-assisted cracking (EAC), dynamic strain ageing (DSA) and degradation mechanisms like hydrogen embrittlement. These effects may happen synchronously or compete with each other (Chopra and Stevens 2018; Higuchi et al. 1997; Que et al. 2019). Furthermore, factors such as multiaxial loading, notching, and material micro-defects can also have a significant impact on fatigue life (Liao et al. 2019, 2020; Bao et al. 2020; Hu et al. 2020; Qian et al. 2010, 2011; Zhong et al. 2020). Based on the research result, the environmental fatigue correction factor (Fen) model which is defined as the ratio of fatigue life in air at room temperature to that in primary coolant environment was developed, the model is then can be used to estimate the effects of primary coolant environments on the fatigue life of RPV material. At present, many different Fen models have been built according to respective situation such as material, operation environment, test condition, etc. (JNES-SS-1005 2011; Chopra and Stevens 2018; Faidy 2012; Gao et al. 2021).

AP1000 NPP is one kind of 3rd generation NPPs that was built in China (Zheng et al. 2016), the RPV material of AP1000 is Chinese A508-3. In order to assess the integrity of the RPV and determine its lifetime in service reasonably, it is necessary to study the fatigue model of Chinese A508-3 steel in a simulated primary coolant environment of AP1000.

The work aims to study the low cycle fatigue behavior of Chinese A508-3 steel in the simulated primary coolant environment of AP1000. Effects of temperature, strain rate and DO on the fatigue life were studied, and then the fatigue model was established, the model of this paper was compared with NUREG6909 model (Chopra and Stevens 2018) which is the model recommended by U.S. Nuclear Regulatory Commission.

2 Experiment procedure

The test material in this paper is a kind of Chinese RPV material named A508-3 steel, which was cut from a RPV forging piece. The main chemical compositions of material satisfied with Chinese National Standard requirements GB15443 (Zheng et al. 2016; Standard 1995), as shown in Table 1. The simulation post welding heat-treatment was performed on the material after cutting from the forging piece, to simulate the real state of the in-service RPV steel. The process of the simulation post welding heat-treatment, which determine the final metallographic structure, is as follows: heating up the material from 300 to 610/620 °C with the heating rate of 55 °C/h, keep the temperature for 30 h, cool it to 300 °C by 55 °C/h, and then cooled in air. The microstructure is bainite (as shown in Fig. 1) with a hardness of 157 Hv.

Fatigue tests were carried out on the Bairoe corrosion fatigue test machine, which is composed of two parts: mechanical test unit and high pressure loop (as shown in Fig. 2). The mechanical test unit consists of a control cabinet, servo motor and the machine frame; the high pressure loop consists of a hydrochemical control circuit, autoclave, the LVDT displacement measurement system and some other components.

The test environment is the simulated AP1000 primary coolant environment. The detailed environment parameters are shown in Table 2. The test temperature is 25–321 °C, the pressure is 15.5 MPa, the water medium is deionized water solution with 2.2 ppm LiOH and 1200 ppm H_3BO_3, pH is 6–7 at room temperature, DO is 0.01 to 8 ppm, and the conductivity is 20–35 μS/cm. The other fatigue parameters are determined after referring to ASTM E606 standard, as follows: triangular waveform, the strain ratio is − 1, the strain rate is 0.004–0.4%/s. The fatigue life (N_f) is defined as the number of cycles for tensile stress to drop 25% from its peak value (ISO 2003; Lin 2008).

Fatigue specimens are in a cylindrical shape. The detailed dimension is shown in Fig. 3, specimen

Table 1 Chemical composition of A508-3 steel in wt%

Element	C	Si	Mn	P	S	Cu	Co	As
Content	0.19	0.17	1.41	0.003	0.002	0.03	0.006	0.003
Element	Sn	Sb	Cr	Ni	Mo	V	Al	B
Content	‹0.002	0.0007	0.12	0.74	0.48	0.002	0.016	0.0003

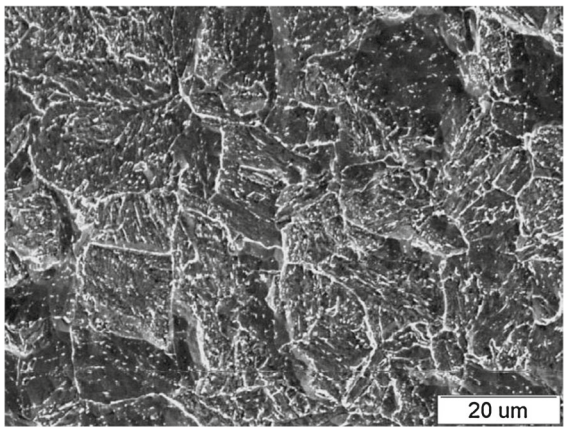

Fig. 1 The metallograph of A508-3 steel observed by SEM

dimension is determined according to ASTM E606 standard (ASTM 2005), with the gauge length of 19 mm and the diameter of 6.35 mm. To measure the strain of fatigue specimen, two collars were set at both ends of gauge length of fatigue specimen, and then strain can be calculated by displacement value of collars which were measured by linear variable differential transformer (LVDT). The stress measuring device is shown in Fig. 4.

3 Results

Figure 5 shows the stress–strain hysteresis loop at half lifetime (50% N_f) when the strain amplitude range is 0.2–0.6% at the strain rate of 0.04%/s in the simulated primary coolant environment of AP1000. It is seen that the hysteresis loop is in spindle shape, with good symmetry; the width of the hysteresis loop increased with the strain amplitude increase, which indicated that the proportion of plastic strain amplitude increases with the increase of strain amplitude. Figure 6 shows the relationship between cycles and peak stress of Chinese A508-3 of the strain amplitude from 0.2 to 0.6%. It can be seen that the initial peak stress increases by 40.2% as the strain amplitude increased from 0.2 to 0.6%, while fatigue life decrease as the strain amplitude increased. For the specimens with large strain amplitude (above 0.25%), as the number of cycles increased, the peak stress increased rapidly at the initial stage and then started to decrease after more than 10 cycles. The increase of the peak stress is more than 10% during the initial stage. In addition, it is seen that during the fatigue process, cyclic hardening, cyclic softening and fatigue instability occurred. While for the specimens with small

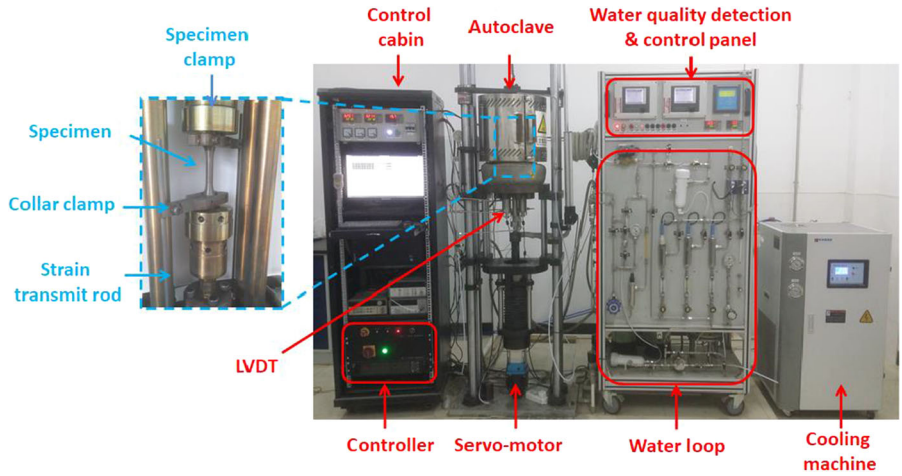

Fig. 2 Corrosion fatigue system with high-temperature and high-pressure environments

Table 2 Environment parameters of fatigue test

Parameters	Primary coolant of AP1000 (Gao et al. 2021)	Test
Temperature	280–321 (°C)	25 ~ 321 (°C)
Pressure	15.5 (MPa)	15.5 (MPa)
DO	5 ~ 100 (ppb)	0.01 ~ 8 (ppm)
pH control agent	2.2 (ppm) LiOH + 1200 (ppm) H_3BO_3	2.2 (ppm) LiOH + 1200 (ppm) H_3BO_3
Conductivity	20–35 (μS/cm)	20–35 (μS/cm)
pH	5–7	6–7

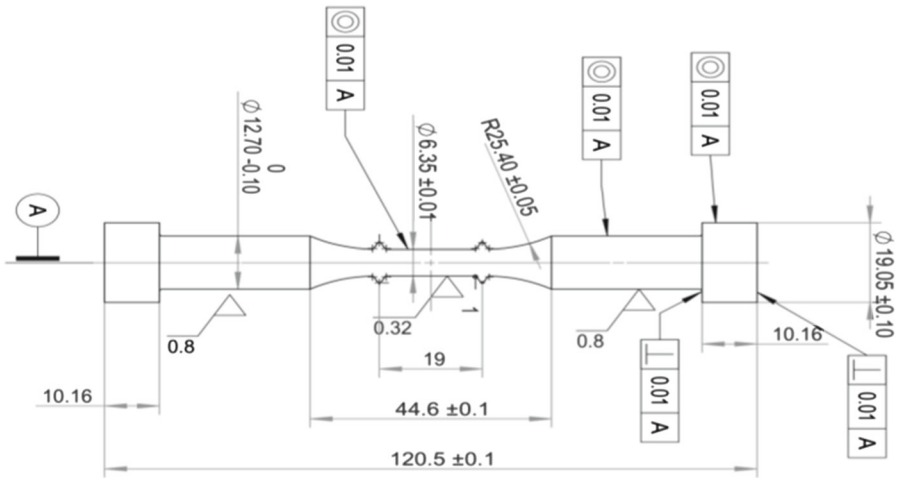

Fig. 3 Fatigue specimen dimension

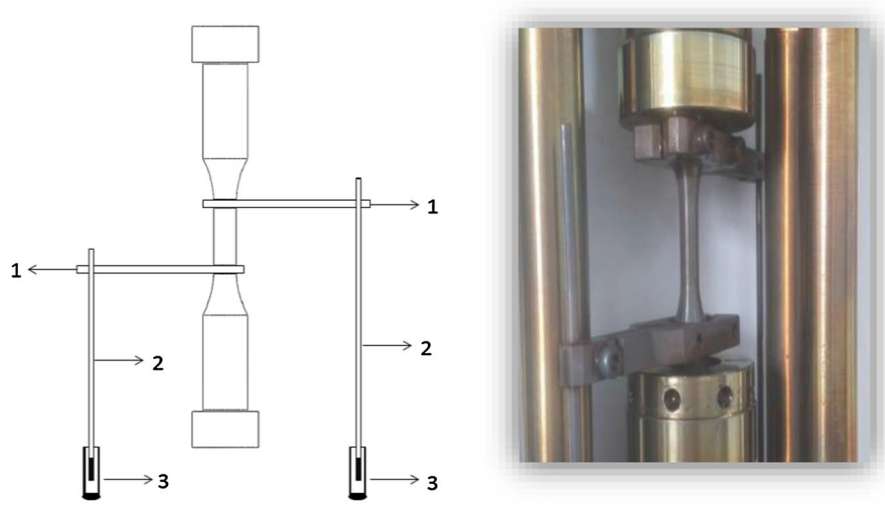

1-Collar clamp, 2-strain guide bar, 3-LVDT

Fig. 4 Stress measuring device in first loop environment

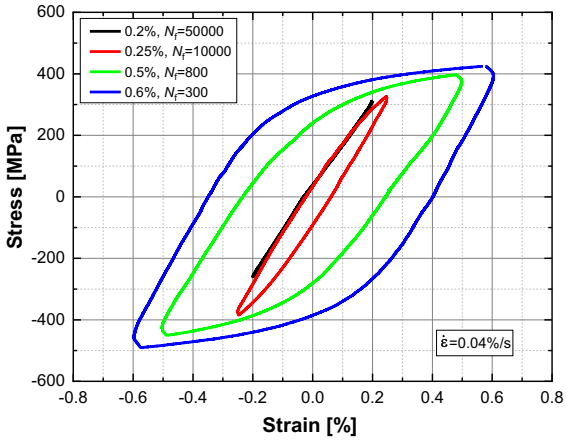

Fig. 5 The stress–strain hysteresis loop at half N_f in the simulated primary coolant environment of AP1000

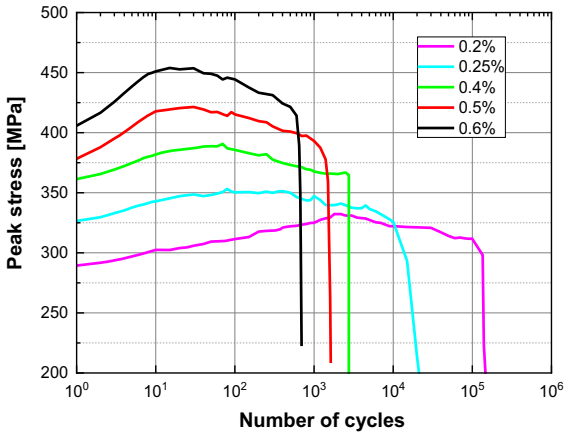

Fig. 6 Relationship between cycles and peak stress of Chinese A508-3 in the simulated primary coolant environment of AP1000

strain amplitude (below 0.25%), the peak stress was stable as the cyclic number increased, the change of the peak stress is less than 10% during the fatigue process, and very slight cyclic hardening or softening was observed. Figure 7 shows the relationship between fatigue life and strain amplitude of Chinese A508-3 under primary coolant environment, and it can be seen that the fatigue life decrease from about 10^5 to 3×10^2, with the strain amplitude increased from 0.2 to 0.6%.

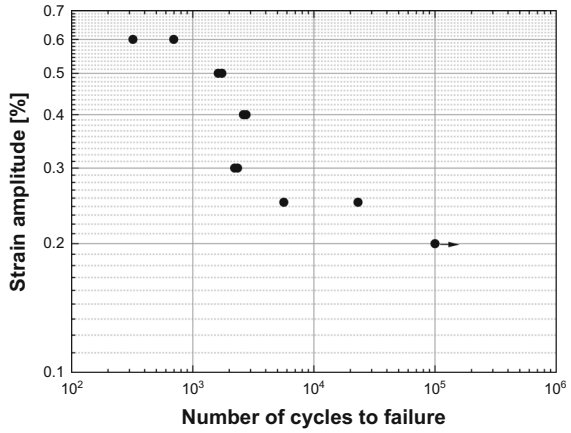

Fig. 7 Relationship between fatigue life and strain amplitude of Chinese A508-3 in the simulated AP1000 primary coolant environment

4 Discussion

As mentioned above, the effect of the primary coolant environment on fatigue life can be expressed by the environmental fatigue correction factor Fen, which is defined as the ratio of the lifetime in air at room temperature to the life in the primary coolant environment. Therefore, in order to predict the fatigue life in the primary coolant environment, not only the fatigue model for room temperature in air condition but also the expression for Fen need to be developed.

4.1 Fatigue life model in air environment

The commonly used fatigue life model is Mason-Coffin model according to the test standards. However, for the sake of engineering application, the Langer model is implemented in the NUREG6909 as the fatigue life model. Therefore, the Langer model is also used to fit the fatigue life model of Chinese A508-3 steel in air environment, the fitted data is tested in the earlier work (Liu et al. 2014), and the fitted model is as follows:

$$\ln(N_f) = 6.255 - 1.620 \times \ln(\varepsilon_a - 0.132). \quad (1)$$

where N_f is fatigue life, ε_a is strain amplitude. Figure 8 shows the fatigue data and life model of Chinese A508-3 in air environment. It can be seen that the present model of Chinese A508-3 is about the same as NUREG6909 model, but overall it is slightly lower than NUREG6909. Figure 9 shows the

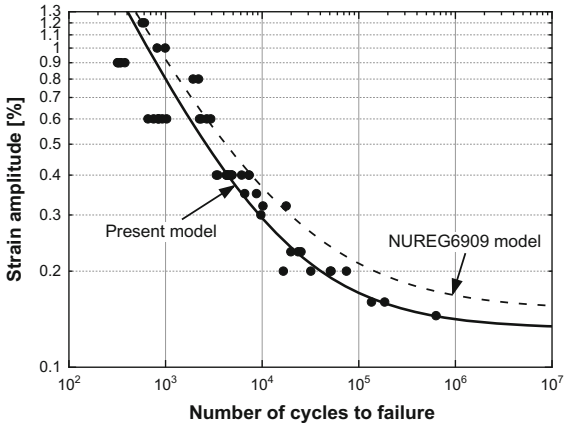

Fig. 8 Fatigue data and life model of Chinese A508-3 in air environment

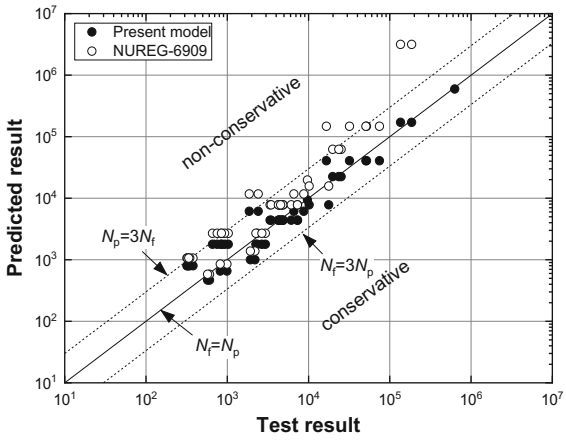

Fig. 9 Comparison of test data and model prediction data of Chinese A508-3 steel in air environment

comparison of test data and model prediction data of Chinese A508-3 steel in air environment. The model prediction data of this paper shows good agreement with the test data and the ratio of prediction data to the test data is within 3. As for comparison, the model prediction data of NUREG6909 is slightly over than the model of this paper. Most of the prediction data is larger than the test data, showing that the prediction is not as accurate as the presented model of this paper.

4.2 Fen and fatigue model in primary coolant environment

Fatigue model in primary coolant environment needs to be established based on Fen and fatigue model in air environment. Fen is usually established based on the effect of different affection factors. Substantial researches confirmed that (JNES-SS-1005 2011; Chopra and Stevens 2018), there are a lot of factors that may affect Fen, i.e. strain rate, temperature, strain rate, DO, S content of the material, load waveform and rate of flow, etc. Among these factors, temperature, strain rate, DO and S content are key factors that should be considered in Fen calculation. As S content of Chinese A508-3 is a fixed value, so the only temperature, strain rate, DO need to be considered in this paper.

4.3 Effect of temperature

The effect of temperature on Fen of RPV is shown in Fig. 10. It can be seen that the logarithm of Fen increases linearly as the temperature increases when the temperature is above 150 °C, and then the effect of temperature on Fen is not significantly below 150 °C. The trend of Chinese A508-3 is similar to other RPV materials (Chopra and Stevens 2018). According to the data of this paper, the relationship between temperature and Fen can be fitted as below:

$$\ln(\text{Fen}) = 0.198 + 0.004 \times T. \quad (2)$$

where Fen is the environmental fatigue correct factor, T is the temperature in °C.

4.4 Effect of strain rate

Figure 11 shows the effect of strain rate on Fen of A508-3 steel. As reported in NUREG6909, the effects

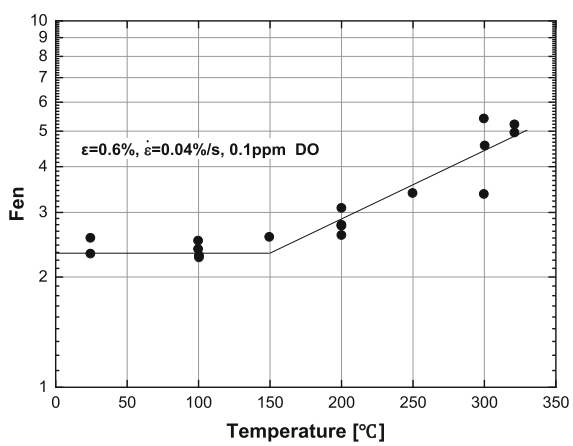

Fig. 10 Effect of temperature on Fen of Chinese A508-3 steel in primary coolant environment

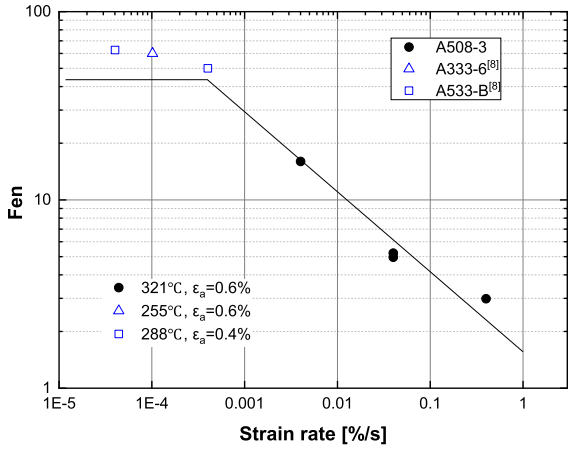

Fig. 11 Effect of strain rate on Fen of different RPV steels in primary coolant environment

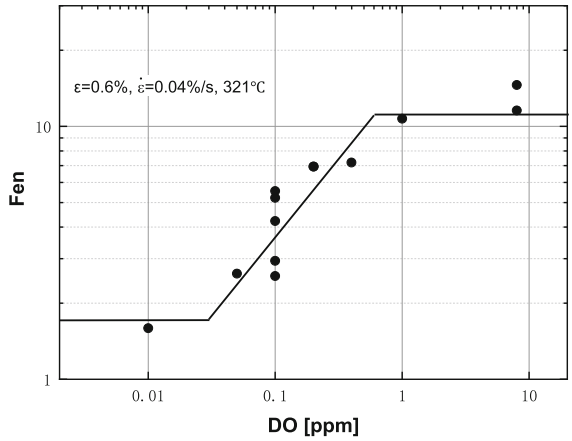

Fig. 12 Effect of DO on Fen of Chinese A508-3 steel in primary coolant environment

of strain rate on fatigue life for the RPV steel would be saturated when the strain rate is below a certain value, and the saturated values were comparable among different RPV steels, such as A333-6, A533-B, A508-3, etc. (Chopra and Stevens 2018). For the sake of studying the saturated value of strain rate, the reference data of NUREG6909 that test below 0.004% were also included in the figure. It can be seen that the Fen increases logarithmically with strain rate decreases when the strain rate is above 0.0004%/s, and then the Fen is a constraint as the strain rate decreases to below 0.0004%/s. The effect of strain rate on Fen of Chinese A508-3 steel is similar to other RPV materials (JNES-SS-1005 2011; Chopra and Stevens 2018). The relationship between strain rate and Fen for Chinese A508-3 steel can be fitted as below:

$$\ln(\mathrm{Fen}) = 0.445 - 0.43 \times \ln(\dot{\varepsilon}). \tag{3}$$

where $\dot{\varepsilon}$ is the strain rate in %/s.

4.5 Effect of DO

Figure 12 shows the effect of DO on Fen of A508-3 steel. It is seen that the Fen decreases logarithmically with decreasing DO in the range of 0.03 ppm to 0.6 ppm, and then the Fen does not change significantly beyond this range. The effect of DO on Fen of Chinese A508-3 steel is similar to other RPV materials (JNES-SS-1005 2011; Chopra and Stevens 2018). The relationship between temperature and Fen for Chinese A508-3 steel can be fitted as below:

$$\ln(\mathrm{Fen}) = 2.72 + 0.62 \times \ln(\mathrm{DO}). \tag{4}$$

where DO is the dissolved oxygen in ppm.

4.6 Fatigue design curve considering the effect of primary coolant environment

According to the discussion of research results (Chopra and Stevens 2018), the Fen of Chinese A508-3 can be express as below:

$$\ln(\mathrm{Fen}) = \mathrm{A} + \mathrm{B} \times \mathrm{X_T} \times \mathrm{X_\varepsilon} \times \mathrm{X_{DO}} \tag{5}$$

where, A and B are coefficients that can be calculated out according to the test data,

$\mathrm{X_T}$, $\mathrm{X_\varepsilon}$ and $\mathrm{X_{DO}}$ are transformed temperature, strain rate, and DO level, respectively, defined as:

$$\begin{aligned}
&\mathrm{X_T} = 0 && (\mathrm{T} \le 150\,^\circ\mathrm{C})\\
&\mathrm{X_T} = (\mathrm{T} - 150) && (\mathrm{T} > 150\,^\circ\mathrm{C})\\
&\mathrm{X_\varepsilon} = \ln(\varepsilon) && (\dot{\varepsilon} \ge 0.0004\%\mathrm{s}^{-1})\\
&\mathrm{X_\varepsilon} = \ln(0.0004) && (\dot{\varepsilon} < 0.0004\%\mathrm{s}^{-1})\\
&\mathrm{X_{DO}} = \ln(20) && (\mathrm{DO} > 0.6\,\mathrm{ppm})\\
&\mathrm{X_{DO}} = \ln(\mathrm{DO}/0.03) && (0.03\,\mathrm{ppm} < \mathrm{DO} < 0.6\,\mathrm{ppm})\\
&\mathrm{X_{DO}} = 0 && (\mathrm{DO} \le 0.03\,\mathrm{ppm})
\end{aligned} \tag{6}$$

According to the test data, the Fen of Chinese A508-3 can be fitted as below:

$$\ln(\mathrm{Fen}) = 0.3143 - 0.00117 \times X_\mathrm{T} \times X_\varepsilon \times X_\mathrm{DO}. \tag{7}$$

Further, by combining the fatigue life model in air environment and Fen, the fatigue life of Chinese

A508-3 in primary coolant environment can be obtained as below:

$$\ln(N_{\mathrm{f}}) = 5.911 - 1.620 \times \ln(\varepsilon_a - 0.132) + 0.00117 \times X_{\mathrm{T}} \times X_{\varepsilon} \times X_{\mathrm{DO}}. \quad (8)$$

Figure 13 shows the comparison of test data and model prediction data of Chinese A508-3 steel in the primary coolant environment. The model prediction data of this paper shows good agreement with the test data and the ratio of prediction data to the test data is within 3. As for comparison, the prediction data of the NUREG6909 model are slightly larger than the model of this paper, indicating that the model of this paper is more accurate in lifetime prediction for Chinese A508-3 steel.

Figure 14 shows the relationship between fatigue life and strain amplitude of RPV steel in different environments. It can be seen that the fatigue life in the primary coolant environment of Chinese A508-3 is overall less than that in air environment, which indicates obvious Environmental Assist Cracking effect exists in the primary coolant environment. Moreover, compared with the NUREG6909 model, the model developed in this paper shows better agreement with the fatigue data of Chinese A508-3 steel, indicating that the presented model is more applicable for fatigue life prediction.

Figure 15 shows the quantitation of fatigue life prediction results. A statistical parameter T_{N} is defined as

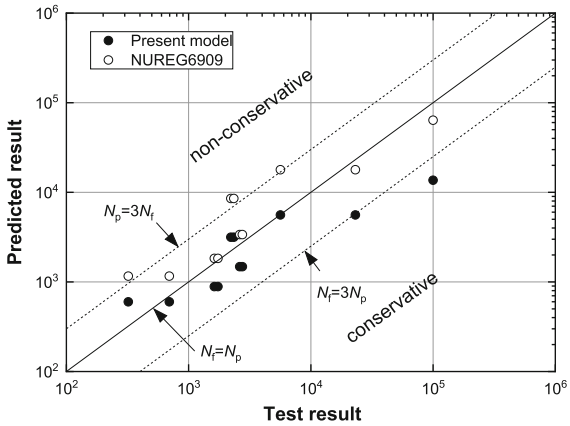

Fig. 13 Comparison of test data and model prediction data of Chinese A508-3 steel in primary coolant environment

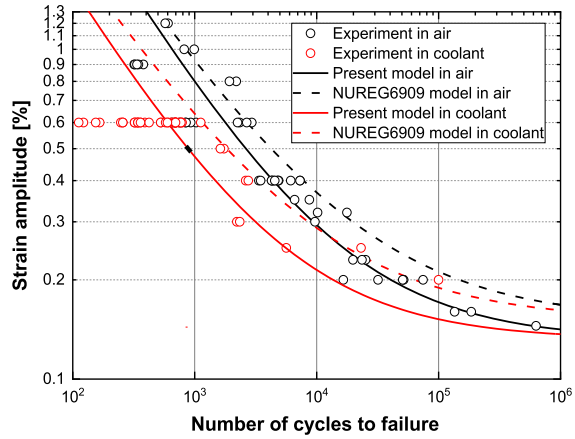

Fig. 14 Relationship between fatigue life and strain amplitude of RPV steel under different test environments

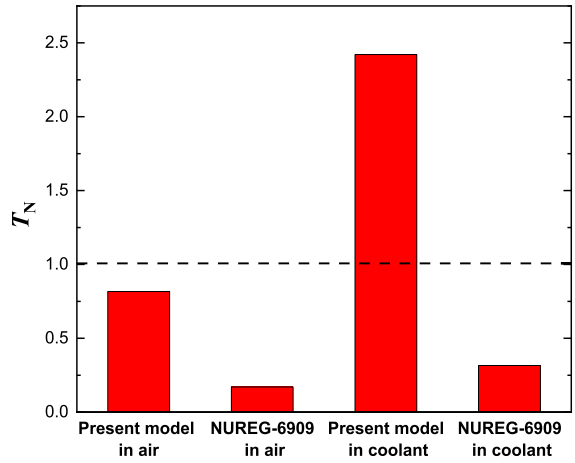

Fig. 15 The quantitative evaluation of the fatigue life prediction results

$$T_{\mathrm{N}} = 10^{\overline{E}}, \quad (9)$$

with

$$\overline{E} = \frac{1}{n}\sum_{i=1}^{n} \log\left(\frac{N_{\mathrm{f},i}}{N_{\mathrm{p},i}}\right), \quad (10)$$

where n is the total number of the compared results, $N_{\mathrm{f},i}$ and $N_{\mathrm{p},i}$ denote the experimental and predicted fatigue life. T_{N} illustrates the comparison of the mean value of experimental and predicted fatigue life. $T_{\mathrm{N}} = 1$ denotes zero difference between experimental mean value and model predictions. $T_{\mathrm{N}} > 1$ means the predicted fatigue life is conservative, and $T_{\mathrm{N}} < 1$ means the predictions are non-conservative.

Compared to the NUREG6909 model, the predicted values of the model presented in this paper are more conservative in both air and coolant environments.

Probability-based *P–S–N* analysis is used to describe the dispersion of the life model. Probabilistic fatigue studies are important for the engineering application of experimental data. Qian and Lei (2019) provided a comprehensive review of existing models for uncertainty analysis. Fatigue failure is a random event for a solid of volume (V) subjected to a cyclic load (S) for a particular number of loading cycles (N). This means that the cumulative probability (P) of fatigue failure is influenced by the cyclic load (S), the number of loading cycles (N), and the specimen size (V). As a result, the cumulative probability (P) of a solid's fatigue failure as a function of cyclic load (S), number of loading cycles (N), and volume (V) can be expressed as follows: $P = F(S, N, V)$.

On the one hand, experimental data collected in a variety of environments, at various strain ratios and temperatures, aids in understanding the fundamental effects of fatigue life. These experimental data, on the other hand, can be utilized to anticipate and extend the life of nuclear power facilities. It is feasible to anticipate the lifetime, which is part of the fatigue design curve, using the *S–N* curve. Furthermore, a probabilistic model of the *S–N* curve provides a lifetime forecast confidence level.

5 Conclusions

In the present work, fatigue tests of Chinese A508-3 were carried out in the simulated primary coolant environment. Effects of temperature, strain rate, and DO on the fatigue lifetime were experimentally investigated. The present fatigue model with the environmental correction factor Fen was proposed and compared to the NUREG6909 model. The conclusions are as below:

(1) During the fatigue tests in the primary coolant, the Chinese A508-3 steel exhibited a cyclic hardening followed by cyclic softening behavior without an obvious cyclic stability region. The fatigue lifetime approximately decreased from 10^5 to 3×10^2, as the strain amplitude increased from 0.2 to 0.6%.

(2) The environmental correction factor Fen is a function of the temperature, strain rate, and dissolved oxygen (DO). Fen decreases as the temperature decreases from 321 to 150 °C, and it decreases as the DO decreases from 0.6 to 0.03 ppm, while it increases as the strain rate decreases from 1 to 0.0004%/s.

(3) The model proposed in the study is more accurate than the NUREG6909 model in fatigue life prediction of Chinese A508-3 steel.

Acknowledgements This work was funded by the National Natural Science Foundation of China (No. 11872364, 12072345), Large-scale Advanced PWR Nuclear Power Plant Major Projects (2018ZX06002008), CAS Pioneer Hundred Talents Program, the Development Project of China Railway (No. N2020J028) and the China Academy of Railway Sciences Corporation Limited (No. 2020YJ115).

References

ASTM E606 (2005) Standard practice for strain-controlled fatigue testing. ASTM International

Bao JG, Wu SC, Withers PJ, Wu ZK, Li F, Fu YN, Sun W (2020) Defect evolution during high temperature tension-tension fatigue of SLM AlSi10Mg alloy by synchrotron tomography. Mater Sci Eng A 792:139809

Byung Ho Lee ISK (1995) Dynamic strain aging in the high-temperature low-cycle fatigue of SA508 Cl. 3 forging steel. J Nucl Mater 226:216–225

C.N. Standard (1995) Pressurized water reactor pressure vessel—the principle of selecting materials and the basic requirements of the materials

Chopra OK, Stevens GL (2018) Effect of LWR coolant environments on the fatigue life of reactor materials, NUREG/CR-6909, Rev. 1

Faidy C (2012) Status of French road map to improve environmental fatigue rules. In: Proceedings of the ASME 2012 pressure vessels & piping conference PVP2012–78805, Toronto, Ontario, CANADA, pp 567–573

Gao J, Liu C, Tan J, Zhang Z, Wu X, Han E-H, Shen R, Wang B, Ke W (2021) Environmental fatigue correction factor model for domestic nuclear-grade low-alloy steel. Nucl Eng Technol 53:2600–2609

Higuchi M, Iida K, Asada Y (1997) Effects of strain rate change on fatigue life of carbon steel in high–temperature water. In: Proc. of symp. on effects of the environment on the initiation of crack growth, ASTM STP 1298. American Society for Testing and Materials, Philadelphia

Hu YN, Wu SC, Withers PJ, Zhang J, Bao HYX, Fu YN, Kang GZ (2020) The effect of manufacturing defects on the fatigue life of selective laser melted Ti-6Al-4V structures. Mater Des 192:108708

ISO 12106 (2003) Metallic materials—fatigue testing—axial-strain-controlled method. International Organization for Standardization

JNES-SS-1005 (2011) Environmental fatigue evaluation method for nuclear power plants, Nuclear energy system safety division. Japan Nuclear Energy Safety Organization

Liao D, Zhu S, Qian G (2019) Multiaxial fatigue analysis of notched components using combined critical plane and critical distance approach. Int J Mech Sci 160:38–50

Liao D, Zhu S, Keshtegar B, Qian G, Wang Q (2020) Probabilistic framework for fatigue life assessment of notched components under size effects. Int J Mech Sci 181:105685

Lin C (2008) Passive safety advanced NPP AP1000. Atomic Energy Press, Beijing

Liu Z, Tong Z, Liang Z (2014) Investigation on low-cycle fatigue property of domestic A508–3 Steel. At Energy Sci Technol 48:127–133

NRC (2007) RG1.207. guidelines for evaluating fatigue analysis incorporating the life reduction of metal components due to the effects of the light-water reactor environment for new reactors. U.S. Nuclear Regulatory Commission

Qian G, Lei W (2019) A statistical model of fatigue failure incorporating effects of specimen size and load amplitude on fatigue life. Phil Mag 99:2089–2125

Qian G, Hong Y, Zhou C (2010) Investigation of high cycle and very-high-cycle fatigue behaviors for a structural steel with smooth and notched specimens. Eng Fail Anal 17:1517–1525

Qian G, Zhou C, Hong Y (2011) Experimental and theoretical investigation of environmental media on very-high-cycle fatigue behavior for a structural steel. Acta Mater 59:1321–1327

Que Z, Seifert HP, Spätig P, Zhang A, Holzer J, Rao GS, Ritter S (2019) Effect of dynamic strain ageing on environmental degradation of fracture resistance of low-alloy RPV steels in high-temperature water environments. Corros Sci 152:172–189

S.I. (1992) ASME Boiler And Pressure Vessel Code, Rules for construction of nuclear powerplant components. American Society of Mechanical Engineers, New York

Yang W (2000) Reactor material science. Atomic Energy Press, Beijing

Zheng M, Jinquan Y, Jun S, Tian L, Wang X, Qiu Z (2016) The general design and technology innovations of CAP1400. Engineering 2:97–102

Zhong W, Qian G, Tong Z, Wu W, Zhu S, Wang C (2020) Fatigue model of domestic 316LN steel in simulated primary coolant environment of CAP1400. Int J Fatigue 130:105297